

Oberlin

## Digital Commons at Oberlin

---

Honors Papers

Student Work

---

1968

### A Two-Part Research Report: Xray Florescence Methods

David Walker

*Oberlin College*

Follow this and additional works at: <https://digitalcommons.oberlin.edu/honors>



Part of the [Geology Commons](#)

---

#### Repository Citation

Walker, David, "A Two-Part Research Report: Xray Florescence Methods" (1968). *Honors Papers*. 11.  
<https://digitalcommons.oberlin.edu/honors/11>

This Thesis is brought to you for free and open access by the Student Work at Digital Commons at Oberlin. It has been accepted for inclusion in Honors Papers by an authorized administrator of Digital Commons at Oberlin. For more information, please contact [megan.mitchell@oberlin.edu](mailto:megan.mitchell@oberlin.edu).

Department of Geology  
Oberlin College  
Oberlin, Ohio 44074

A TWO-PART RESEARCH  
REPORT  
SUBMITTED AS PART  
OF THE REQUIREMENTS FOR DEPARTMENTAL HONORS  
IN GEOLOGY

David Walker

May 18, 1968

## INTRODUCTION AND ACKNOWLEDGEMENTS

The work of this project was divided between analytical chemistry by xray fluorescence techniques and geologic interpretation of a series of PreCambrian crystalline rocks from the contact aureole of the Stillwater igneous complex in the Beartooth Mts. of Montana. The former was needed for the latter. There are two sections to the report which correspond to the double thrust of the research.

I wish to thank Dr. William R. Skinner who provided the rocks and thin sections used in this report, who supervised the work, and who provided stimulating discussion on the petrology. Also Dr. James L. Powell who offered constant aid and advice in the xray work and other quantitative aspects of the project (besides providing a good running account of the isotope scoreboard). Also Dr. S. Stephen Streeter who provided an invaluable series of services with his computer programming facility. He is also to be thanked for supplying instruction and material to use in applying statistical techniques to the data, interpretation of the results, and a program subroutine to draw graphs. Also to the Oberlin College Computer Center for many hours of expensive computer time. Further indebtedness is mentioned in the body of the paper. I also wish to thank my fiancée Sandy Holder for the use of her typing skills (and patience).

## XRAY FLUORESCENCE METHODS

The purpose of this section of the paper is to document the xray fluorescence methods used to obtain the data reported on Rb, Sr, Fe, Mn, and Ti concentration values in a later section of the paper. Also, a new instrumental approach and a new analytical method are suggested for the analyses of the elements of atomic number 21-26 (Sc-Fe). All methods involve estimation of the mass absorption coefficient ( $\mu$ ) of the rock.

## Sample preparation:

Whole-rock specimens were prepared for xray analysis by grinding to a fine powder and pressing that powder into a disc-shaped briquette suitable for mounting directly in the xray beam. Specimens of the SZ series were slabbed with a water lubricated table saw, trimmed of peripheral weathering zones, and then reduced to pebble-chip size in a rough, cylindrical steel mortar. Specimens of the 67 series were merely fractured open, trimmed of peripheral alteration, and then reduced to pebble-chip size in the same way. The resulting chips were then ground for 5 minutes in a Spex Industries Shatterbox. This procedure netted about 100-200 grams of powder for each specimen. The Shatterbox is believed not to shed iron powder from itself into the specimen powder during grinding. To confirm this another sample of SZ-15 was ground by hand in a porcelain mortar and analysed for iron. The results of xray analysis showed that the porcelain-ground sample was, if anything, a 1/10% richer in iron than the Shatterbox-ground sample, and hence the Shatterbox could not be shedding any significant or measurable amount into the specimens. The difference in results may be due to slight sample inhomogeneities as the chips were from different sections of the rock.

A teaspoon of the resultant powder was pressed into boric-acid-supported



disc briquettes in apparatus analogous to that described by Damon(1966,p14). The pellet-compressing cylinder apparatus was loaded to 8kpsi, allowed to adjust about 15 seconds, and then loaded to 26kpsi in the hydraulic press. After the load had equilibrated about 1 minute, the load was let off very gradually with extreme caution observed to insure even unloading, lest the rock powder split out of the boric acid. The briquette was identified and the boric acid surfaces sprayed with clear Krylon plastic. The specimen was then ready for xray analysis.

#### RB & SR ANALYSES:

The method of Reynolds (1963) was employed in the xray analyses of these two elements. This approach employs the empirical linear relation between the reciprocal of the intensity of the Molybdenum-excited Compton scattered peak and the mass absorption coefficient ( $\mu_\lambda$ ) of the material. Compton scattered xrays are generated by incoherent scattering of impinging xrays on the bombarded material. A change in wavelength ( $\Delta \lambda$ ) results so that the Compton scattered radiation diffracts to a different  $2\theta$ . As the atomic number of the matrix decreases, the proportion of scattered xrays of the Compton type increases relative to coherent scattering. Matrices of low atomic number have low  $\mu_\lambda$  and also matrix absorption of the resultant incoherently scattered xrays would decrease for matrices of low  $\mu_\lambda$ . Intensity of the Compton scattered radiation would be expected to increase with decreasing atomic number matrix (decreasing  $\mu_\lambda$ ) or conversely the reciprocal of the intensity of the Compton scattered radiation would be expected to increase with increasing  $\mu_\lambda$ . Reynold's (1963) chief contribution was to demonstrate that this relationship was linear and useful under certain conditions.

To illuminate those conditions and to prepare for later discussion, digressive reference is made to the study of Hower (1959). Hower noted that the variation of the relative mass absorption coefficients with wavelength (the ratio of the mass absorption coefficients of two matrices at some wavelength) was such that the relative mass absorption coefficients were constant between the wavelengths of the mass absorption edges of the major matrix constituents. As Hower noted that iron is usually the heaviest major matrix element, matrices should have constant relative mass absorption coefficients for all wavelengths in the region beyond the Fe absorption edge. This region (called Region I by Hower) includes the K $\alpha$  spectra of Ni and those heavier including Mo, Rb, and Sr. In the region (Region II) between the absorption edge of Fe and the next heavier major matrix constituent's absorption edge - usually Calcium - a different relative mass absorption coefficient obtains for all wavelengths in that region. This curious "step-like" variation of relative mass absorption coefficient with wavelength arises from the similar rate of increase of  $\mu_{\lambda}$  with  $\lambda$  for all the major matrix elements. This similar rate of increase obtains on opposite sides of the elements absorption edge. Hower demonstrates this by taking logarithms, plotting, and measuring slopes. The reason for the discontinuity in relative mass absorption at the major element's absorption edge is that the two matrices containing that element may, in general have different amounts, and thus have their rate of increase of total  $\mu_{\lambda}$  upset by different amounts by the absorption edge of the element in question. If the amount of the element in each matrix was the same, the relative absorption discontinuity would be 0. If the amount of the element present differed in each matrix, the relative absorption discontinuity would depend both on the difference in amount between the two, and on the amounts actually present.

This can be seen by formulating  $D = \frac{\mu_1}{\mu_2} - \frac{\mu'_1}{\mu'_2}$  which is the difference in relative mass absorption coefficients.  $\mu_1$  and  $\mu_2$  are the mass absorption coefficients of matrix 1 and 2 respectively figured on one side of the absorption discontinuity and  $\mu'_1$  and  $\mu'_2$  are the mass absorption coefficients of the matrices figured just on the other side of the absorption discontinuity. Using the additivity of fractional mass absorption coefficients:

$$\mu_1 = \mu_A \cdot A_1 + \mu_L \cdot \frac{L_1}{L_1} \quad (1)$$

and

$$\mu'_1 = \mu'_A \cdot A_1 + \mu'_L \cdot \frac{L_1}{L_1}$$

and similarly for  $\mu_2$  and  $\mu'_2$  where:

$A_1$  is the weight fraction of the element with absorption edge at wavelength in question in matrix 1.

$\mu_A$  and  $\mu'_A$  are the mass absorption coefficients of this element on the opposite sides of the absorption discontinuity.

$L_1$  is the weight fraction of the remainder of the matrix  $1 = (1 - A_1)$ .

$\mu_L$  is the mass absorption coefficient of the remainder of matrix 1 at the wavelength in question.

As a result:

$$D = \frac{(A_1 - A_2)}{aA_2^2 + bA_2 + c} \quad (2)$$

where  $a$ ,  $b$ , and  $c$  are constant functions of  $\mu_A$ ,  $\mu'_A$ , &  $\mu_L$ .

Obviously the size of the relative absorption discontinuity depends not only on the difference but also on the amount of element at the absorption edge present in each matrix. If the amounts of the absorptionally disruptive element are equal in the two matrices ( $A_1 = A_2$ ) then  $D=0$  as noted before.

Returning to the limitations of Reynolds' Compton scattered estimation of  $\mu_\lambda$ , we can see that if  $\mu_\lambda$  is determined for one wavelength of Compton scattered radiation, the use of this determination of  $\mu_\lambda$  in finding the relative mass absorption coefficient, the goal, will be appropriate for that

and the same element absorption edge will be the same

region defined by major element absorption edges which contains the  $\lambda$  for which  $\mu_\lambda$  was determined. For the case of MoK $\alpha$  primary radiation and the Compton scattered radiation in Region I of Hower, the  $\mu_\lambda$  determined by Reynolds' method is useful in obtaining the relative absorption coefficient with some standard to which comparisons will be made for Rb and Sr which are also in the Region I. Reynolds (1963, p1133) notes the general equation regarding xray intensities and element concentrations:

$$Z = \frac{\mu_\lambda}{k} \cdot IZ_{K\alpha} \quad (3)$$

where

$Z$  = concentration of  $Z$  in sample

$IZ_{K\alpha}$  = intensity of the  $Z K_\alpha$  radiation

$\mu_\lambda$  = mass absorption coefficient of the sample at the wavelength  $ZK_\alpha$

$k$  = instrumental constant.

By comparison with a similar equation for a standard matrix of known  $Z$  and  $\mu_\lambda$  and a measurable  $IZK_\alpha$

$$Z_{std} = \frac{\mu_{\lambda std}}{k} \cdot IZK_{\alpha, std} \quad (4)$$

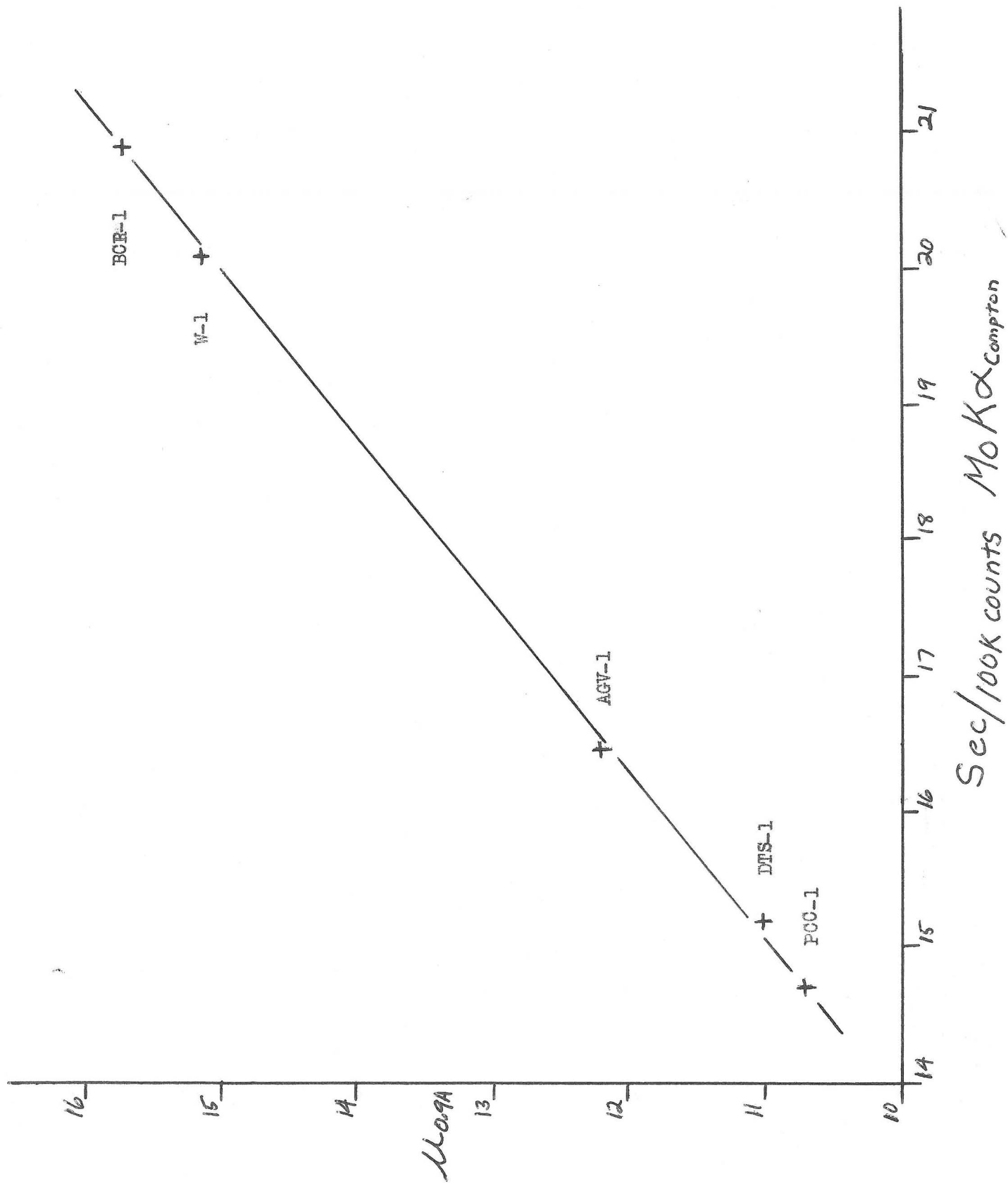
and dividing (3) by (4), we remove the instrumental constant  $k$ :

$$Z = \frac{\mu_\lambda \cdot IZK_\alpha}{\mu_{\lambda std} \cdot IZK_{\alpha, std}} \cdot Z_{std} \quad (5)$$

Reynolds (1963, pii34-5) is a bit misleading with his limitations on this equation by claiming that it is not applicable to Hower's Region II. As he himself implicitly admits in Reynolds (1967) by applying it, the expression is valid as long as the  $K_\alpha$  radiation and the  $\mu_\lambda$  apply to the same region defined by major element absorption edges. (We shall neglect enhancement effects for the remainder of the paper.) Thus it is feasible to determine a  $\mu_\lambda$  for Region I on the basis of Compton scattering of Region I radiation

Reynolds-type curve/ Data taken on March 18, 1967

Figure 1



and apply it to Rb and Sr lines of sample and standard since Hower has assured us that the relative absorption coefficient  $\mu_{\text{sample}} / \mu_{\text{standard}}$  is constant throughout Region III. One cannot however apply Region I Compton scattered determinations to Region II elements because of the absorption discontinuity between the two areas. One could apply the formula if he could obtain the  $\mu$ 's for Region III. More will be said about this later.

The actual analytical work for this study was done by establishing a working curve like Reynolds' of reciprocal Compton scatter intensity vs. known mass absorption coefficient for the USGS standards each day (see Fig.1),

PCC-1	10.71	Values of $\mu$ at 0.9A calculated from USGS analyses and data in Liebhaksky, et.al (1960).
DTS-1	11.02	
AGV-1	12.20	
W-1	15.13	
BCR-1	15.71	

and fitting a line of least squares to the data. Mass absorption coefficients for the samples were determined by substituting reciprocal Compton scattered intensity into the least squares linear formula. Rb and Sr ppm were then calculated by measuring the background-corrected intensities of the Rb and Sr peaks of unknown and standard and applying the general formula (5) for comparing standard and unknown.

USGS standard G-1 was used as the standard for comparison. Values used:

$$\begin{aligned}\mu_{0.9A} &= 9.89 \\ \text{ppm Sr} &= 250 \\ \text{ppm Rb} &= 220\end{aligned}$$

A few statistical calculations were made on each specimen to determine the standard counting error and the limit of detection of each element in that specific matrix. Following Jenkins and deVries (1967, p96-101) the formula selected to calculate the counting error of the net intensity of the element's measured peak is

$$\sigma_d = \sqrt{\frac{R_p}{T_p} + \frac{R_b}{T_b}} \quad (6)$$



where:  $R_p$  and  $R_b$  are the counting rates of the peak and background measurements and  $T_p$  and  $T_b$  are the counting times of the peak and background measurements.  $\sigma_d$  is the standard counting error on the net intensity rate.

The criterion used to compute the limit of detection is that the peak signal should be 3 times the standard deviation of the background above the background.

$$LMDT = \frac{3(\sigma_{\text{background}})(\text{ppm}_Z)}{(\text{net intensity})} \quad \text{where:} \quad (7)$$

LMDT is the limit of detection for the matrix in ppm,  $\sigma_{\text{background}}$  is the standard deviation of the background counting rate ( $\sqrt{R_b/T_b}$ ), net intensity refers to the background-corrected signal for element  $Z$ , and  $\text{ppm}_Z$  is the amount of element  $Z$  in that specimen.

A computer program in FORTRAN IV language was written to perform all the calculations described above plus a few others described in the program options. The program, named RBSR, is in the computer appendix to this paper and copies of the source decks are on file in the Oberlin College department of geology. This holds for the rest of the programs referred to in this paper.

The instrumental work was carried out on a General Electric XRD-5 xray spectrometer. A LiF crystal was used for diffracting with a thallium-activated NaI scintillation counter for a detector. A Mo target emission tube was used to provide primary excitation radiation. Mo is optimal for Rb-Sr work because, as already noted, its Compton scattered radiation is in Region I as are Rb and Sr  $K_{\alpha}$  lines, and also because excitation efficiency for Rb and Sr is great. Mo has its intense characteristic lines with wavelength close to the absorption edges of Rb and Sr but on the shorter wavelength - high absorption - side of these edges (optimum condition for high excitation efficiency). The Mo tube was operated at 51 KV and 30 MA, being allowed to stabilize about an hour before use. LiF is a good crystal to use because it provides suitable resolution without catastrophically reducing intensities. The  $2\theta$  required is small, therefore intensity losses due to absorption losses directly into the crystal are minimal. The crystal was periodically aligned during the analytical work. The Rb and Sr concentrations found in this study were generally small with resultant low peak intensities. The problem then was not with resolution but with counting rates. For this reason a collimator with a relatively wide (.010") slit replaced a relatively narrow (.005"). The justification for this instrumental change which reduced resolution comes from the added benefit of increased peak height. Jenkins and deVries (1967, p100) warn against taking

peak/background ratio maximization as a criterion of analysis superiority.

They suggest, rather than the quantity

$$(\sqrt{R_p} - \sqrt{R_b}) \approx \text{Merit Factor} \quad (8)$$

should be maximized (where  $R_p$  and  $R_b$  are the counting rates of peak and background respectively).

For the purposes of this study the wide collimator gave the superior merit factor; for example on a typical specimen W-1:

Merit Factors for W-1 counting rates

Element	Wide Collimator	Narrow Collimator
Sr	10.0	6.9
Rb	1.2	.8
Ti	4.7	2.3

In every case the low counting rates dictated that the wide-slit collimator gave the better figure of merit and so the wide collimator was used (except for the first half of the first run for Fe, Mn, and Ti in the SZ series).

The number of counts taken on peaks and backgrounds was usually 10,000 however in cases where increased precision was desired in those specimens selected for Rb-Sr age determination, 100,000 counts were taken. 100,000 counts were always taken on the Mo Compton scattered peak.

The precision and accuracy attained with this method compare favorably with analytical methods of far more difficulty when samples have concentrations a few times the limit of detection. In cases where the concentration approached the limit of detection, the results were considerably less precise. For ordinary specimens, 3 determinations of Rb and Sr were made taking 10,000 counts. For SZ-1 thru SZ-7 one run was made taking 100,000 counts. The average limits of detection were about 7ppm for each element. For other rocks of the Boulder River metasediment suite that were used for age determination (including 2A, 12, 20, 13A, and 13C of the SZ series), from 4 through 13 determinations were made taking 100,000 counts on peaks and backgrounds, depending upon the level of concentrations present. This procedure gave a limit of detection of 2.5 ppm. For these samples used in age determinations, sample preparation was done by Dr. Wm. R. Skinner and Mr. H.C. Bates and the extra xray determinations were performed by Mr. H.C. Bates.

A computer program called MEAN to perform the calculations to determine the mean values, standard deviations, and percentage standard deviations of

analysis output from program RBSR or any set of replicate Rb-Sr analyses <sup>written.</sup> ~~WBSA~~  
This program is in the appendix.

The actual mean values obtained are reported in a later section of this paper. When concentrations were of such a low level that a negative value was calculated, 0 is recorded. When Sr becomes low and Rb/Sr "blows up" suitable adjustments are made in reporting data values. The values obtained for each analysis and the output of the mean program for the replicate measurements are on file in the appendix. Values below 10 ppm have small significance for the SZ series and 67 series while values below 5 ppm have small significance for the Boulder River metasediment suite.

A good idea of the accuracy and precision of the method can be gained from the data for W-1 which is a standard with matrix of typical  $\mu$  for this study. Note that the low Rb value leads to lower precision in the determination.

W-1 data (19 measurements)

Quantity	calculated mean	accepted value	$\sigma$	typical $\sigma_d$	$\sigma$ %	typical $\sigma_d$ %
Rb	21.5	22*	.90	1.2	4.17	5.3
Sr	188	180*	3.39	1.5	1.80	.8
$\mu_{0.9A}$	15.10	15.13**	.10		.67	

\*Fleischer (1965)

\*\*calculated, see above

$\sigma$  and  $\sigma$  % here refer to the standard deviation from the mean calculated for a number of measurements and to the % standard deviation:

$$\sigma = \sqrt{\frac{\sum (x - \bar{x})^2}{n-1}} \quad (9)$$

$$\sigma \% = 100 \cdot \sigma / \bar{x} \quad (10)$$

where:

$\bar{x}$  is the average of the values of measurements,  $x$ , and

$n$  is the number of measured  $x$  values.

$\sigma$  is not the same as  $\sigma_d$  of equation (6) which is the standard counting error. The discrepancy between  $\sigma$  and  $\sigma_d$  should be a measure of the instability of the machine. The comparison of  $\sigma$  and  $\sigma_d$  in the above is not conclusive in establishing a value for  $\sigma_{\text{machine}}$ . This is due to the fact that the above  $\sigma$  values are not simple counting error but have incorporated

also the uncertainties in the Reynolds curve and in the standard G-1 measurements.

A determination of  $\sigma_{\text{equipment}}$  could better be done by considering the measurements of the Compton scattered peak. According to Liebafsky et al (1960), p277), when the standard deviation of a measurement exceeds the standard counting error significantly then other errors are present besides counting errors. These errors are in the technique used or in the equipment.

For the Compton scattered peak 100,000 counts (N) were always taken so the standard counting error ( $S_c$ ) is

$$S_c = \sqrt{N} \quad (11)$$

following Liebafsky(p272) and Jenkins and deVries(p92); or in relative percent

$$\epsilon_c \% = \frac{100}{\sqrt{N}} = \frac{100}{\sqrt{100000}} = .316\% \quad (12)$$

where  $\epsilon_c \%$  is relative % counting error.

To figure out a standard deviation, the number of seconds were used since the number of counts was constant. The resultant % relative standard deviation of the actual measured time  $\epsilon_t \%$  is calculated according to equations (9) and (10) where time values are substituted for x.  $n = 19$ .

$$\sigma = \sqrt{\frac{\sum (2x - \bar{x})^2}{n - 1}} = .194 \text{ seconds} \quad (13)$$

$$\epsilon_t \% = \sigma \cdot 100 / \bar{x} = \frac{.194 \cdot 100}{22.436} = .865\% \quad (14)$$

Now  $\epsilon_t \%$  is the actual observed relative standard deviation of the measurement and  $\epsilon_c \%$  is the expected relative standard deviation of the counting error. The discrepancy is a measure of machine instability and technique mishandling ( $\epsilon_{\text{equipment}}\%$ ). Jenkins and deVries (1967,p102-4) give the relation required to find  $\epsilon_{\text{eqp}}\%$ . Suitably modified it becomes:

$$\epsilon_{\text{equipment}} \% = \sqrt{(\epsilon_t \%)^2 - (\epsilon_c \%)^2} = \sqrt{(.865)^2 - (.316)^2} \quad (15)$$

$$\epsilon_{\text{equip}} \% = .805\% \approx .81\%$$

This means that on good measurements taken from day to day one can expect a variation in results due to the equipment factor alone of .81%. It is of interest to note that the values of  $\sigma$  % for the values of  $\mu_{0.9A}$  calculated from these measurements is only .67% -- a result of the fact  $\mu_{0.9A}$  is

calculated by reference to numbers which also are subject to the instrumental variation. The fact that  $\epsilon_{\text{equip}} > 5\%$  for  $\mu_{0.9A}$  indicates that the variation is systematic for all the measurements used in determining  $\mu_{0.9A}$  from day to day. That is to say that while the values for PCC-1, W-1, etc. may vary instrumentally by .81% from day to day, they vary in a systematic way so that the calculations made from their relationships do not vary that much. They all vary up or down from day to day in the same direction so that  $\mu_{0.9A}$  calculated from the curve does not suffer variation to the extent of the variation of each point but only to the extent of the variation of one point versus another. This systematic machine variation from day to day is justification for establishing a new Reynolds  $\mu_{0.9A}$  curve each operating day. This exposition on day to day systematic machine variation is consistent with the often observed <sup>fact</sup> that precision of measurements on sample analysed on the same day is greater than if the samples are analysed on different days.

These variations are small, however, compared to those observed in the calculated values of Rb and Sr. The values obtained for 19 measurements on W-1 of  $\sigma_{\text{Rb}}\% = 4.2$  and  $\sigma_{\text{Sr}}\% = 1.8$  are typical of the  $\sigma\%$  values obtained from 3 thru 13 measurements on specimens with similar concentrations suitably above the limit of detection. The precision tends to be better for those measurements recording 100,000 counts for age determination. The close agreement of the observed values with the accepted values for W-1 speaks well for the accuracy of the method.

#### FE, MN, & TI ANALYSES:

The newly published method of Reynolds (1967) was used to determine  $\mu$  for Region II of Hower which contains the  $K_{\alpha}$  lines of Fe, Mn, and Ti. Once  $\mu$  was determined by this method, equation (5) could be applied for any element in Region II. W-1 was chosen as the concentration standard and as the standard used in the Reynolds calculation of  $\mu$  for Region II. Reynold's equation was used intact:

$$\mu_{1.94}^u = \frac{(15.67)(\mu_{0.9}^u)(\text{IFe}^s)}{(2.062)(\text{IFe}^s) + (\text{IFe}^u)} \quad (16)$$

where  $\mu_{1.94}^u$  and  $\mu_{0.9}^u$  refer to the mass absorption coefficients of the unknown at 1.94A and 0.9A;  $\text{IFe}^s$  and  $\text{IFe}^u$  are the net counting intensities of the Fe peak in standard and unknown. This equation uses the values of W-1:

mass absorption Fe	.0775
8	
1.94	78.36
Fe	
1.94	74
0.9	



<u>W-1</u>	weight fraction Fe	.0778
$\mu_{1.94}^s$		78.36
$\mu_{1.94}^{Fe} \approx \mu_{0.9}^{Fe}$		74
b		7.6

where b is a quantity to be discussed at length later.  $\mu_{0.9}^u$  was determined by the method of Reynolds (1963) described above.

Once  $\mu_{1.94}$  was known for an unknown, this value was employed in equation (5) along with the appropriate net counting rates measured on standard and unknown. W-1 was used as a reference standard for concentrations also. The values used as accepted values for concentrations (and the units in which they are reported):

<u>W-1</u> *	Fe	11.30	weight % as $Fe_2O_3$
	Mn	1320	ppm
	Ti	6400	ppm

In

\*Fleischer (1965)

In measuring intensities 100,000 counts were accumulated on the Fe  $K_{\alpha}$  peak and 1,000 on each side of the background. For both Mn and Ti peaks and the associated backgrounds, 10,000 counts were taken.

A computer program named FEMUG (in appendix) was developed to expedite the necessary calculations plus the statistical limit of detection and standard counting error and % relative counting error calculations. Each analysis was performed induplicate and the results fed into another program (AMGIS, in appendix) which calculated average values and standard deviations for measured quantities observed in duplicate on a number of samples. The formulas for these statistical quantities:

$$\sigma_p = \sqrt{\frac{\sum (X_1 - X_2)^2}{2N}} \quad (17)$$

$$\sigma_p\% = \sigma_p \cdot 100 / \bar{X} \quad (18)$$

where  $X_1$  and  $X_2$  are the values obtained when measuring the same quantity two different times, N is the number of samples subjected to this duplicate measurement procedure, and  $\bar{X}$  is the arithmetic mean of all the X values.

$\sigma_p$  is the standard deviation for pairs of measurements and  $\sigma_p\%$  is the relative % standard deviation for the pairs of measurements.



Tabulated values for  $\sigma_p\%$  for the analysis of 40 samples indicate reasonably good precision for the xray measurements. The mean values are reported later in this paper while the individual values are on file with the rest of the computer output.

Quantity	$\mu_{0.9A}$	$\mu_{1.94A}$	Fe	Mn	Ti
$\sigma_p\%$	.62	.81	.75	3.19	2.36

(N = 40)

An average of  $\sigma_p\%$  for Mn and Ti is 2.77%. Now an average of the relative % counting error for Mn and Ti on the same measurements is only 1.82%. Using equation (15) to find the  $\epsilon\%$  for factors other than counting error (approximate since  $\sigma_p\%$  is related to other measurements indirectly also):

$$\epsilon\% = \sqrt{(2.77)^2 - (1.82)^2}$$

(19)

$$\epsilon\% = 2.08\%$$

Qualitatively, this number is a good deal larger than the .81% calculated for the strict  $\epsilon_{\text{equipment}}\%$  from the Compton scattered peak measurements. One reason for this is that we are dealing in average calculated values rather than in sigmas for direct measurements; but instead we could calculate a similar  $\epsilon\%$  for element determinations which would be attended by the same collection of uncertainties and would serve as a better comparison. Compare  $\epsilon\%$  for W-1 Sr (data above):

$$\sqrt{(\sigma\%)^2 - (\sigma_d\%)^2} = \sqrt{(1.80)^2 - (.8)^2} = 1.61\% \quad (20)$$

which is a lower  $\epsilon\%$  than for Mn and Ti. Recalling that these Mn and Ti measurements were taken with only 10,000 counts vs. 100,000 for the Compton scattered and most of the W-1 Sr measurements, might lead one to suspect that this factor increased the variability. One would expect this increased variability to show in  $\sigma_p\%$  and  $\sigma_c\%$  but not in the  $\epsilon\%$  for things besides counting errors. (Note that the element that was suitably high above the detection limit in W-1 - Sr - had a total  $\sigma\%$  of 1.80% compared to the "other-factors-besides-counting  $\epsilon\%$  of 2.08% for elements Mn and Ti which are also suitably above the detection limit.) The problem is to be found by noting the exceedingly small counting rates observed in Mn and Ti which necessitated long counting times to accumulate the fewer counts. Long term

machine variation coupled with day to day variation probably account for the large  $\epsilon_{\text{equip}}\%$ . The W-1 measurements were made on only a few different days while the Mn and Ti values were obtained on many operating days. Also, and perhaps of most importance, the Rb-Sr standard G-1 was run often with W-1, thereby eliminating the effects of long term machine drift; whereas the Mn and Ti standard, W-1, was run only once each operating day because of the time-consuming nature of the low peak intensity measurements. For the measurements on the Compton scattered radiation and W-1 the time taken to collect the counts was short and so long term machine drift was not a problem.

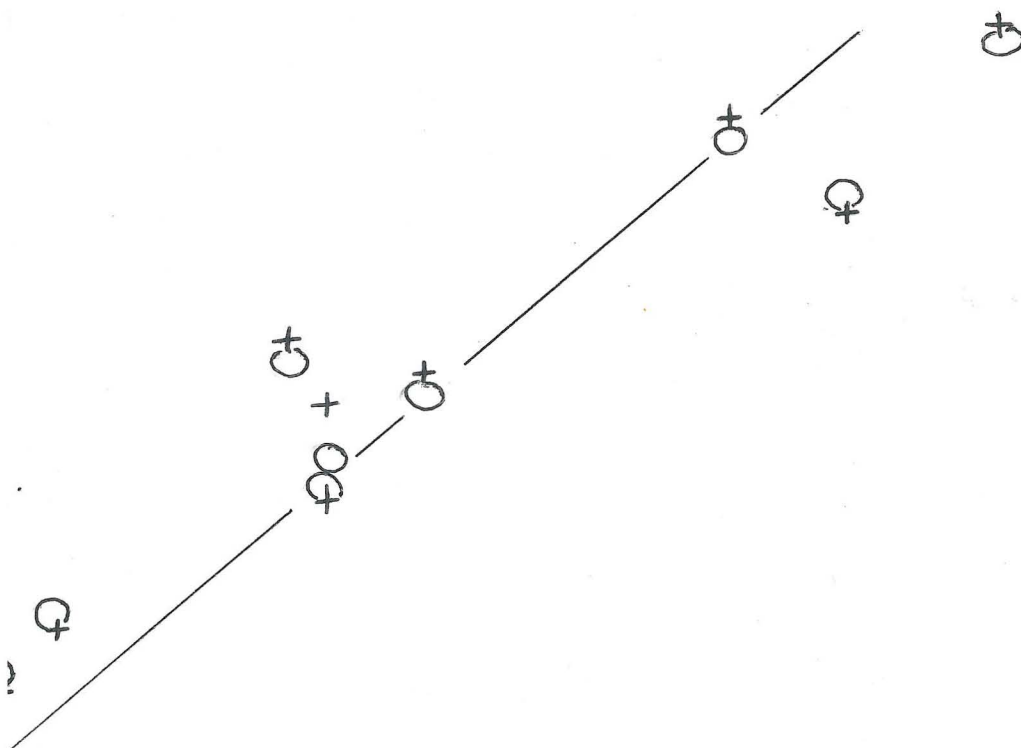
The evil of low peak intensities is perpetrated by the following agents:

- a) Inefficient excitation of Mn and Ti (Mo tube was operated under the same conditions mentioned for Rb-Sr work above).
- b) Larger loss of signal strength by absorption into diffracting crystal at larger  $2\theta$  than Rb, Sr, and  $\text{MoK}_{\alpha}$  Compton peaks.
- c) High mass absorption coefficient of the sample in the longer wavelength region of Mn and Ti.

None-the-less, precision for this method of analysis is quite respectable, and certainly sufficient for the purposes of this study. One of the new methods suggested below would alleviate a), the insufficient excitation. We are now ready to examine the accuracy of Reynolds' method and suggest two possible alternatives.

#### DISCUSSION OF TRANS-FERRIC XRAY WORK:

The work of Reynolds presents an easy and unencumbered way to determine mass absorption coefficients for Region II of Hower on the long wavelength side of the iron absorption edge. The precision, as we have seen, is quite respectable as xray methods are wont to be. To discuss the accuracy we must digress quickly to restate some general concepts pertaining to mass absorption coefficients. Mass absorption coefficients of the constituents of a material



Data from U.S.G.S., Boulder River, and  
Pomona College analyses.

Xray work  
Apr. 18, 1968

sed Iron Content

6.85

8.72

10.58

TABLE 1

Specimen	FE cps $\times 10^{-2}$	Wt. % Iron	$M_{0.98}$	$M_{2.08}$	$B = \left( \frac{M_{2.0}}{M_{0.9}} \right)$	
G-1	22.4	1.36	9.89	75.29	7.61	U.S.G.S. standards
W-1	13.58	7.79	15.31	85.01	5.62	
G-2	37.3	1.86	10.14	74.56	7.35	
GSP-1	54.4	2.97	11.12	75.62	6.80	
AGV-1	94.1	4.65	12.20	76.93	6.31	
PCC-1	154.0	5.70	11.10	58.86	5.30	
DTS-1	158.0	6.02	11.51	60.21	5.23	
BCR-1	168.0	9.28	15.71	81.52	5.19	
SD-15	192.4	9.86	14.59	67.80	4.65	Boulder River analyses
SG-50A-1	150.2	7.36	13.92	76.09	5.47	
SA-93	175.3	7.11	12.75	67.22	5.27	
SH-59A	156.0	7.30	12.91	67.64	5.24	
SG-47	214.0	10.58	15.05	67.68	4.50	
PC-1	23.2	1.33	9.75	73.94	7.59	Pomona College standards
PC-2	47.2	2.71	10.74	74.74	6.96	
PC-3	27.9	1.26	9.79	74.92	7.65	
PC-4	58.4	2.50	10.61	74.93	7.06	
PC-5	107.5	5.13	12.76	79.04	6.19	
PC-6	90.8	4.62	12.06	76.47	6.34	

$$k = 1.46 \times 10^5$$



fraction of  $i$  in the matrix. This result is stated by Liebhafsky (1960,p15). By this formula, the expected  $\mu_{\lambda}$  of some sample that has been analysed chemically can be determined by looking up mass absorption coefficient values for the constituents at some wavelength. Once  $\mu_{\lambda}$  is known we are in a position to learn more from the general equation for xray intensity (3), here restated:

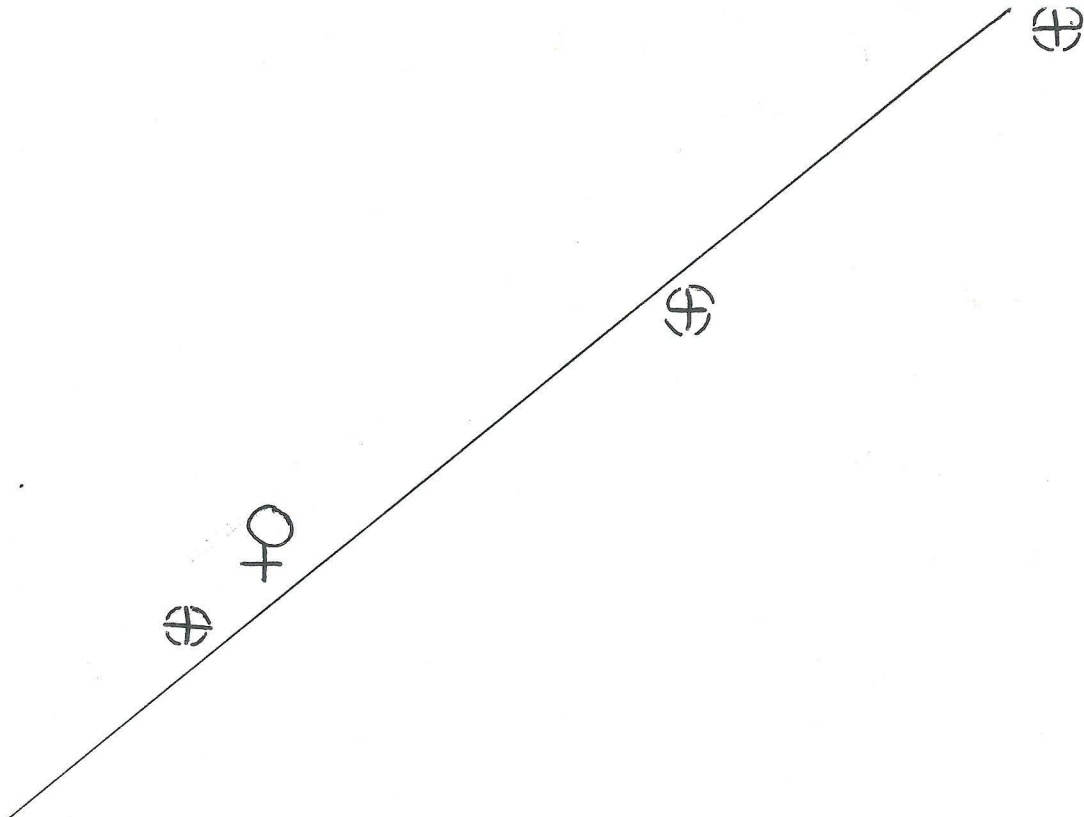
$$Z = \frac{\mu_{\lambda}}{k} \cdot IZK_{\alpha}$$

Since  $Z$  and  $\mu_{\lambda}$  are known from the analysis and  $IZK_{\alpha}$  can be measured directly, the value of  $k$  can be determined. (see table 1)  $Z$  plotted against  $\mu_{\lambda} \cdot IZK_{\alpha}$  should be a straight line through the origin with slope  $1/k$ . Any deviations from linearity could be attributed to:

- 1) Counting error in  $IZK_{\alpha}$  (negligible in good measurements).
- 2) Non-correspondence of  $Z$  or  $\mu_{\lambda}$  analysis values with rock sample due to inaccuracies in the analysis or imprecision in the reference constituents  $\mu$ 's.
- 3) Enhancement effects which are of no importance in the case of iron studied.

2) is thought to be most important since data from different days is the same and there is no major element to enhance iron.

From analyses of 19 rocks, the necessary data for such a plot was calculated. The values of constituent mass absorption coefficients were selected from Liebhafsky (1960,p314-5) for 0.9A and for 2.0A (a convenient wavelength in Region II for which there is direct data). Data was measured for the iron  $K_{\alpha}$  peak intensity, the element of interest in Region II, and tabulated in Table 1 with the  $\mu_{\lambda}$  and other values of interest later. The first 8 rocks are standards issued by the USGS that have been determined by wet chemical and other means. The next 5 rocks are from the Boulder River metasediment suite and were analysed by H. Wiik in Finland for Dr. A. Poldervart of Columbia (deceased). They were kindly provided with their analysed results by Dr. Wm. R. Skinner. The Last 6 rocks are xray analysed "secondary standards" based on the USGS standards issued by Pomona College. These and the ~~USGS~~ standards with analyses were kindly provided by Dr. J.L. Powell. Figure 2 is a plot of iron content from the analyses against the quantity  $(\mu_{2.0A} \times IFe)$  where  $\mu_{2.0A}$  was calculated from the analyses and  $IFe$  is the intensity of the iron  $K_{\alpha}$  line (+character). The plot, when extended, does hit the origin and



Data from U.S.G.S. Standards  
Apr. 18, 1968 Xray Work

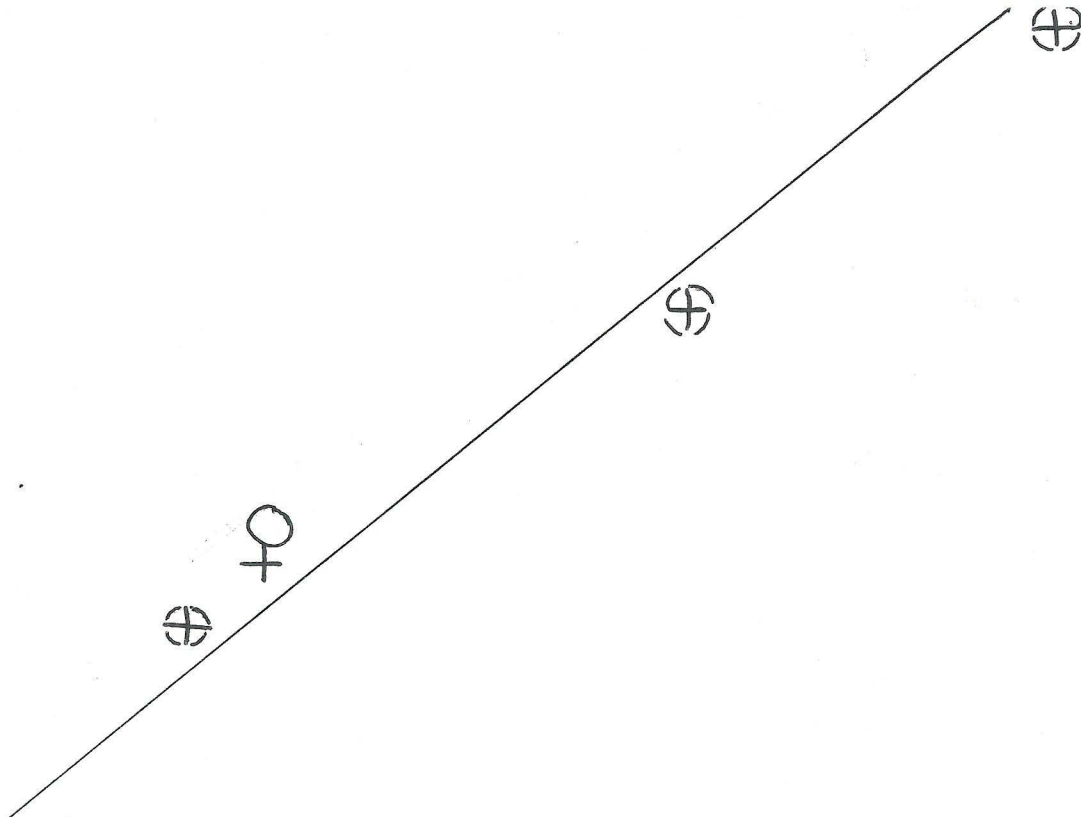
Analysed Iron Content

16.11

17.70

19.28





Data from U.S.G.S. Standards  
Apr. 18, 1968 Xray Work

Analysed Iron Content

16.11

17.70

19.28

appears to be linear. However there is a scatter about the line which is the result of the uncertainties mentioned above. For comparison the quantity (Reynolds'  $\mu_{2.0A} \times \text{IFe}$ ) is also plotted against iron content on the same graph (0 character) where Reynolds'  $\mu_{2.0A}$  is the  $\mu_{2.0A}$  in Region II determined by Reynolds' (1967) method. Reynolds' equation was suitably modified to calculate at 2.0A instead of 1.94A by changing  $\mu^{\text{Fe}}$  to 80, W-1  $\mu_{2.0}$  to 85.01, and b to 8.59. We need not worry that 2.0A is not the  $\text{FeK}_{\alpha}$  wavelength because of Hower's study. Practically the same scatter is observed in the 0 character plot, point for point. This indicates that the values of analysed  $\mu_{2.0}$  must be close to the values of Reynolds'  $\mu_{2.0}$  which certainly speaks well for the method. The scatter about the line remains to be explained more fully.  $\mu_{2.0}$  calculated from the analyses depends on the accuracy of the analyses, and the accuracy to which the  $\mu$ 's of the constituents are known. One would expect the plot for Reynolds'  $\mu_{2.0}$  to show a bit less scatter since the  $\mu$ 's are subject to and in a sense "standardized by" the uncertainties in W-1's analysis rather than all the uncertainties in all the analyses. (Both types of  $\mu$  are subject to the uncertainties in the constituent's  $\mu$ 's)) This tightening of scatter is probably reflected in the 0 character being on the "line side" of the + character in 13 out of 19 cases. Scatter because of  $\mu_{2.0}$  variation would seem to be minor. If both methods of finding  $\mu_{2.0}$  give the same scatter it would be more reasonable to expect the larger component of the scatter was derived from the other axis, analysed iron content. Unless all the analyses have large random errors, it is hard to upset  $\mu_{2.0}$  calculated from the analyses with small errors in one or two constituents. If however analysed iron content didn't correspond quite closely to the rock sample, then scatter in the plot would be directly introduced in proportion to the non-correspondence of rock and analysed iron value. The two most important sources of scatter appear to be analytical inaccuracies and possible constituent  $\mu$  inaccuracies. One would expect the better analyses to show less scatter. Figure 3 is a similar plot of both types of ( $\mu_{2.0} \times \text{IFe}$ ) against analyses iron content for the 8 USGS standards. The scatter is a good deal less than for all 19 rocks, justifying our confidence in these analyses as superior to the other two sets. (Actually a plot for the Pomona College standards was almost as good except for PC-2.) The scatter at the low end of the curve has a large effect on the answers obtained by the Reynolds' method "percentage wise". This is painfully apparent for G-1, perhaps the best analysed rock in the series of standards



TABLE 2

SPECIMEN	Reynold's method			observed		accepted values	
	MU 0.9A	MU 2.04A	PC IRON	FE	CPS	ANALY. MU 2.0A	IRON
G-1	9.70	76.81	1.16	2239.	75.29	1.36	
W-1	15.15	86.25	7.90	13576.	85.01	7.79	
G-2	10.26	77.28	1.94	3728.	74.56	1.86	
GSP-1	11.21	79.97	2.94	5440.	75.62	2.97	
AGV-1	12.29	78.06	4.96	9410.	76.93	4.65	
PCC-1	10.99	59.85	6.22	15405.	58.86	5.70	
DTS-1	11.56	62.37	6.65	15795.	60.21	6.02	
BCR-1	15.66	82.57	9.36	16803.	81.52	9.28	
SD-15	13.92	69.51	9.03	19239.	67.80	9.86	
SG-50A-1	13.52	74.31	7.53	15018.	76.09	7.36	
SA-93	13.29	68.90	8.15	17533.	67.22	7.11	
SH-59A	12.81	69.45	7.31	15590.	67.64	7.30	
SG-47	14.62	69.71	10.07	21403.	67.68	10.58	
PC-1	9.78	77.24	1.21	2318.	73.94	1.33	
PC-2	10.75	78.44	2.50	4724.	74.74	2.71	
PC-3	10.05	78.12	1.47	2787.	74.92	1.26	
PC-4	10.75	75.70	2.98	5841.	74.93	2.50	
PC-5	12.76	78.13	5.67	10752.	79.04	5.13	
PC-6	11.67	74.80	4.58	9077.	76.47	4.62	

besides W-1.

The case of G-1 deserves special attention in that the failure to reproduce Reynolds' results which correspond well with the accepted values is notable.

<u>G-1</u>	Quantity	average value this report	accepted value	<u>reported</u> <u>accepted</u>
	$\mu_{2.0}$	74.72	75.29	.99
	Wt. % Fe	1.10	1.36	.81
	Mn ppm	144	230	.63
	Ti ppm	1210	1500	.81

At first this was thought to mean that the technique was not good, however one must note that the  $\mu_{2.0}$  obtained was very close to the one expected on the basis of the analysis calculation. This would seem to indicate that (as long as the basic equations between intensity of radiation,  $\mu_p$ , and element concentration hold) the failure lies in the non-correspondence of the iron in our sample of G-1 with the accepted values. This must also be the case with Mn and Ti which show anomalously low values even though the  $\mu_{2.0}$  determined is close to the accepted value. Since a 1% error in the  $\mu_{2.0}$  cannot produce a 20-30% error in calculated concentration values, we are forced to conclude that our sample of G-1 does not have the same amount of Fe, Mn, and Ti as the normal G-1 analysis. Perhaps an accidental separation of some of the magnetite could account for such a lowered value for the 3 elements. The agreement of Reynolds' method's results with accepted values for the rest of the USGS standards is assuring. (see Table 2)



To measure the quality of a procedure in determining values near the accepted value, the term collective uncertainty is introduced and defined in an analogous fashion to standard deviation of pairs of measurements except that the accepted value makes up one value of the pair of measurements.

$$CU = \sqrt{\frac{\sum (X_o - X_a)^2}{2 \cdot N}} \quad (22)$$

$$CU\% = CU \cdot 100 / \bar{X}_a \quad (23)$$

CU and CU% are the collective uncertainty and % relative collective uncertainty respectively.  $X_o$  are observed measured values,  $X_a$  are accepted values, and N is the number of specimens for which CU is being calculated. This quantity behaves like the standard deviation. When CU is high then there is poor agreement of observed and expected values. CU is chosen to be a measure of accuracy for a method of analysis.

An alternate method of data treatment following an analogous example from Damon (1966, pl7) for Rb and Sr, would be to determine  $\mu_{2.0}$  by Reynolds' (1967) method and then making a plot of (Reynolds'  $\mu_{2.0}$  · IFe) like Figure 2 or 3 vs. analysed iron content for a few well known standards. A least squares line could be fit to those points and then unknowns determined by calculating (Reynolds'  $\mu_{2.0}$  · IFe) and referring to the least squares line to find the corresponding iron concentration. This method has the advantage of simultaneously making comparisons with a wide range of standards ( an advantage, of course, if the standards are well known) rather than just one. It however requires extra xray time to do more standards. This technique shall be designated Reynolds  $\mu_{2.0}$  (multiple standards)

to distinguish it from the Reynolds (1967) technique as published. Table 3 compares the CU% of these two techniques for iron analysis and also some others which will be discussed shortly. Each technique was tried using all 19 rocks and then just the USGS standards. In each case the USGS standard's results had the lower CU%, supporting our faith in the superiority of these analyses over the other two groups. For the multiple standard treatment, the group in question was analysed by comparison with the curve which that group alone generated.

TABLE 3 Compiled Collective Uncertainties (CU%)

Method	19 rocks	USGS Standards
Reynolds (1967)	7.62	5.70
Reynolds (multiple standards)	7.33	4.07
B vs. IFe	9.16	4.63
B (multiple standards)	8.89	4.43

The values for the method of least CU% are here in Table 4.

TABLE 4

MULTIPLE STANDARD CURVE OF ANALYSED IRON VS IFE\* MU2.0  
 MU CALCULATED BY REYNOLDS METHOD(1967)  
 SLOPE = 0.64430860E-05 INTERCEPT = 0.44796996E-01

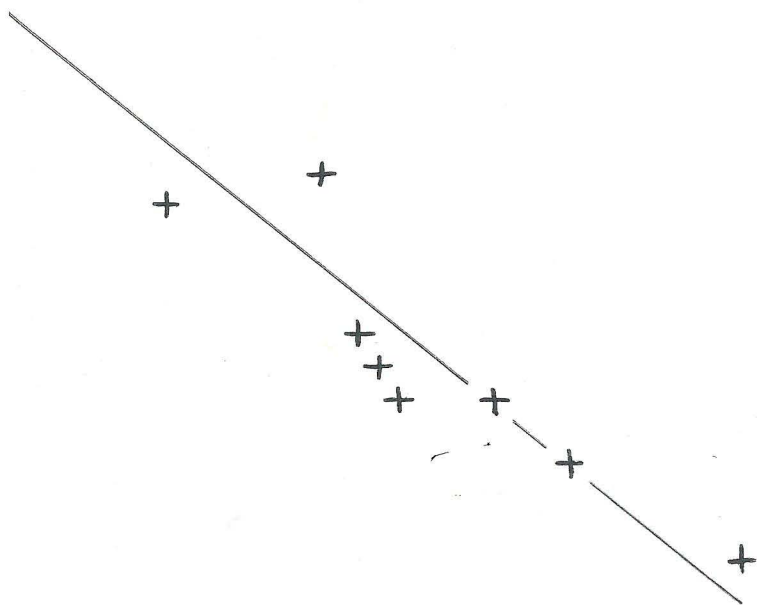
SPECIMEN	CALC. FE	ANALYS. IRON
G-1	1.15	1.36
W-1	7.59	7.79
G-2	1.90	1.86
GSP-1	2.85	2.97
AGV-1	4.78	4.65
PCC-1	5.99	5.70
DTS-1	6.39	6.02
BCR-1	8.98	9.28



The computer program (IRON) that performed the calculations for this table and drew a number of graphs is on file in the appendix. The output attached to it contains tables of values obtained for each specimen by each method and the slopes and intercepts of the various least squares curves. Subroutine LSQ was written to handle the least squares analyses and subroutine DELSQ was written to handle the CU and CU% calculations. Both are compiled with IRON.

It seems that the Reynolds claim of accuracy (vicinity of 4%) is substantiated, especially when one considers that the c.a. 6% which is calculated for CU% includes the very substantial error in G-1. Reynolds also claims that the variation arises from "uncertainties in published values for mass absorption coefficients" to which we should add uncertainty in the analyses as mentioned above. We should also mention the miniscule error introduced by the assumption of constant relative mass absorption coefficients (Hower) which is probably less than 1%. Reynolds also includes variability of  $b$  as a cause of error. In his method,  $b = \mu_{II} / \mu_I$  where II and I refer to suitable wavelengths in Hower's Region I and II to which the two  $\mu$ 's can be referred. These  $\mu$ 's are for materials which have no absorption edge in the wavelength range II-I. He uses this  $b$  in his method with the explicit assumption that  $b$  is nearly a constant given the two wavelengths II and I, and with the implicit assumption that there are not major amounts of elements present in the matrix with absorption edges in range II-I except iron (i.e. low Mn, Cu, Zn, etc). Deviations from these conditions are possible and a method was discovered which eliminates the necessity of these assumptions.

Data from U.S. G.S., Boulder River, and  
Pomona College Standards



Xray work  
Apr. 18, 1968

13.74

17.57

21.40